Available online at www.sciencedirect.com
SCIENCE DIRECT
Journal of Power Sources 155 (2006) 375–380
JOURNAL OF POWER SOURCES
www.elsevier.com/locate/jpowsour

Electrochemical properties of $LiCoO_2$ thick-film cathodes prepared by screen-printing technique

Seung-Tae Lee [a], Shin-Wook Jeon [a], Byung-Joo Yoo [a], Seung-Don Choi [b], Hyeong-Jin Kim [b], Sung-Man Lee [a,*]

[a] *Department of Advanced Materials Science and Engineering, Kangwon National University, ChunCheon Kangwon-do 200-701, South Korea*
[b] *Battery Research Institute, LG Chemical Limited, Taejon 305-380, South Korea*

Received 20 February 2005; accepted 13 May 2005
Available online 1 August 2005

Abstract

A screen-printing process is used to prepare thick Zr-incorporated $LiCoO_2$ (Zr–$LiCoO_2$) films up to 20 μm. The sol slurry used for the screen-printing consists of a Zr–$LiCoO_2$ sol and the Zr–$LiCoO_2$ powder. The microstructure and morphology of the films are investigated. After a thermal treatment, crack-free crystalline films are obtained. The electrochemical properties of the thick films are investigated in a half-cell with a Li-metal anode and in a full-cell with a Fe/Si multilayer film anode. Excellent cycleability is observed. Incorporation of 5 wt.% Ag powder into the sol slurry for screen-printing improves the electrochemical performance such as the charge–discharge coulombic efficiency. This is attributed to enhanced electrical conductance. It is found, however, that the degree of utilization of the electrode material decreases with increasing film thickness.

Keywords: Screen printing; Thick films; Lithium-ion batteries; Cathode; $LiCoO_2$

1. Introduction

In recent years, there has been an increasing interest in all-solid-state rechargeable lithium batteries with thin-film configurations because of their wide range of applications in microelectronics, sensor technology, and microelectromechanical systems (MEMS) [1–7]. Preparation of thin films for electrode and electrolyte materials and the choice of these materials are crucial factors for the fabrication of rechargeable microbatteries.

Crystalline $LiCoO_2$ films have shown excellent electrochemical properties as cathodes for thin-film rechargeable batteries. To date, $LiCoO_2$ cathode films have generally been prepared by physical deposition methods (e.g., sputtering [7–18], laser ablation [19,20]) and chemical methods (sol–gel [21,22]). These thin-film techniques demonstrate the capability of producing films of typically around 1 μm thickness.

With the sol–gel method, in general, films of up to 0.3–1 μm are deposited in a single layer and thicker films are achieved by multiple depositions. These processes are time-consuming and costly for fabrication. Moreover, the development of cost-effective thick-film technologies is required for many applications of microbatteries because the capacity of lithium-ion microbatteries basically depends on the thickness of the cathode films.

Screen-printing is a traditional process that is suitable for fabricating films with thicknesses of larger than 10 μm [23]. Its characteristics of low cost and easy operation make the process suitable for industrial production.

This study is devoted to the development of such a process for the fabrication of thick films of cathode materials and to the investigation of their electrochemical properties as negative electrodes for Li rechargeable batteries. The powder

* Corresponding author. Tel.: +82 33 250 6266; fax: +82 33 242 6256.
E-mail address: smlee@kangwon.ac.kr (S.-M. Lee).

0378-7753/$ – see front matter © 2005 Elsevier B.V. All rights reserved.
doi:10.1016/j.jpowsour.2005.05.065

used for this purpose is Zr-incorporated $LiCoO_2$, prepared by a sol–gel process.

2. Experimental

Fine Zr-incorporated $LiCoO_2$ (hereafter called Zr–$LiCoO_2$) powders were prepared by a sol–gel method, in which lithium acetylacetonate $LiCH_3Co$–$CHCOCH_3$ and cobalt(II) acetate tetrahydrate $Co(CH_3CO_2)_2{\cdot}4H_2O$ in the Li:Co ratio of 1:1 was used as solutes, and a mixture of 2-methoxyethanol and acetic acid was used as the solvent. The precursor sol for ZrO_2 was obtained by mixing zirconium *n*-propoxide (70% solution in propanol) with an equimolar quantity of acetylacetone, which is used as a stabilizer. The precursor sol was added to the $LiCoO_2$ sol, and the resultant precursor solution was stirred with a magnetic stirrer for 10 h in a nitrogen atmosphere. The precursor powders were obtained from the solution by drying in a vacuum oven at 80 °C for 24 h and then at 120 °C for 12 h. The powders were calcined at 800 °C for 2 h after pre-calcining at 400 °C for 1 h in air. The chemical composition of the final compound was determined by inductively coupled plasma (ICP) analysis. The resulting composite powders have Li:Co and Zr:Co molar ratios of 0.97 and 0.015, respectively.

Thick films have been prepared by a screen-printing technique followed by adequate heat treatment. The Zr–$LiCoO_2$ powder was dispersed into the Zr–$LiCoO_2$ sol to obtain a paste for thick-film deposition. The powders and the sol are identical in composition. The paste was mixed by ball-milling in a planetary mill (Pulverisette-7, Fritsch) for 2 h at 200 rpm. For some pastes, 5 wt.% (relative to the Zr–$LiCoO_2$ powder mass) Ag powders (around 2.5 μm) were added in order to enhance the electrical conductivity. The paste thus prepared was screen-printed on to a platinum-coated alumina substrate. Each film was preheated at 150 and 380 °C for 1 h and the final heat treatment was at 750 °C for 1 h.

The microstructure and the thickness of the resultant film were examined with a field emission scanning electron microscopy (FESEM). Structural identification was performed by means of X-ray diffraction (XRD) with Cu Kα radiation.

Glass beaker-type cells were used to evaluate the electrochemical properties of the samples. The electrochemical cell was composed of a lithium metal foil as the counter electrode and a Zr–$LiCoO_2$ thick film as the working electrode. For full-cell testing a Fe/Si multilayered film was used as the anode. Experimental details of preparing the Fe/Si multilayer film have been described elsewhere [24]. The electrolyte was 1 M $LiPF_6$ in a mixture of ethylene carbonate (EC) and diethyl carbonate (DEC) (1:1 (v/v), provided by Cheil Industries Inc., South Korea). All electrochemical tests were performed in an Ar-filled glove box at 30 °C. The cells were galvanostatically charged and discharged at 100 μAh cm^{-2}.

3. Results and discussion

A scanning electron micrograph and the XRD diffraction pattern of Zr–$LiCoO_2$ powders used to make a screen-printing paste are presented in Fig. 1. The particles are spherical with a size around 1 μm. A small extra peak appears in the XRD pattern and is attributable to a trace Co_3O_4 impurity phase. Nanoscale ZrO_2 phase introduced into the $LiCoO_2$ particle could be detected by using transmission electron microscopy. The cycle performance of Zr–$LiCoO_2$ is better than that of bare $LiCoO_2$ (data not shown here). A similar result has been previously reported [25] in which the introduction of TiO_2 into $LiCoO_2$ resulted in a considerable improvement in electrochemical performance of $LiCoO_2$ material. Therefore, Zr–$LiCoO_2$ powders are used here to make a paste for a screen-printing.

The surface image and cross-sectional view of a Zr–$LiCoO_2$ thick film is shown in Fig. 2. The film is screen-printed on to a Pt current-collector coated alumina substrate, followed by post-heat treatment. A crack-free films with a uniform thickness is obtained. The XRD pattern indicates that the films contain a crystalline $LiCoO_2$ phase. In the case of the Ag-doped film, the diffraction peak of Ag is also visible (Fig. 3).

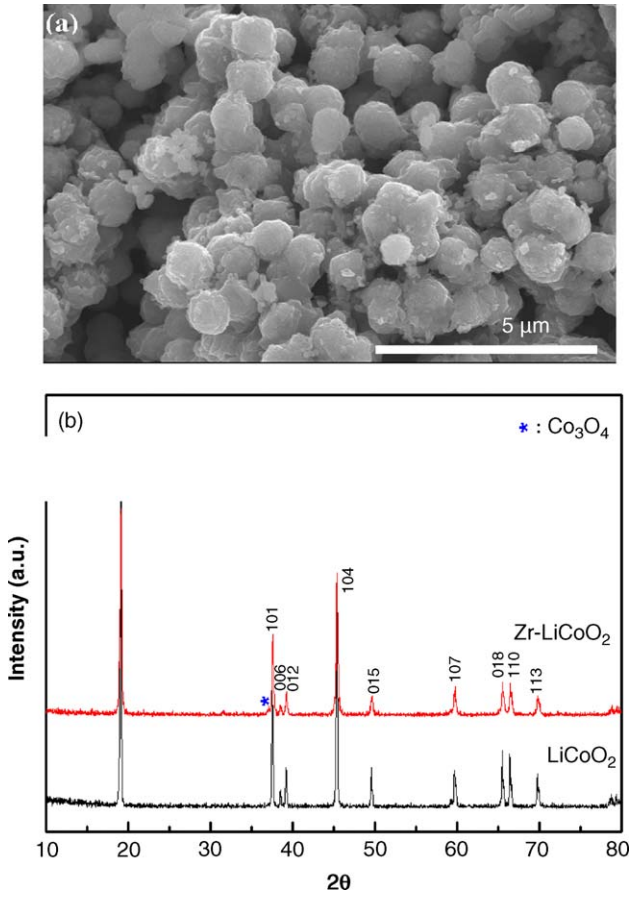

Fig. 1. (a) SEM micrograph and (b) X-ray diffraction pattern of Zr–$LiCoO_2$ powder prepared by sol–gel method.

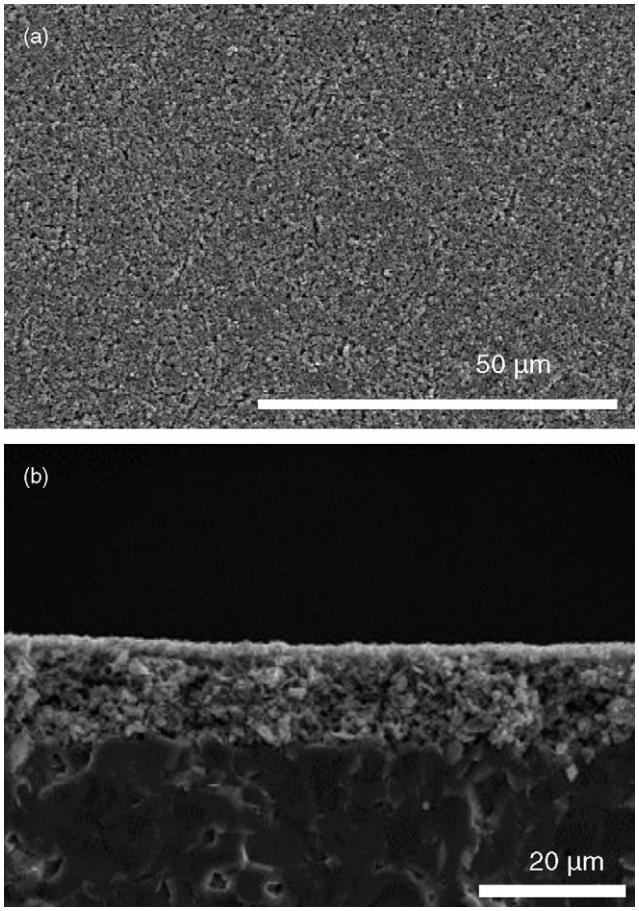

Fig. 2. SEM micrograph of Zr–$LiCoO_2$ film prepared by screen-printing method: (a) surfaces and (b) cross-section of film.

Charge–discharge curves for Zr–$LiCoO_2$ films with/without 5 wt.% Ag powder are given in Fig. 4. These were obtained at a constant current density of 100 μA cm^{-2} between 3.0 and 4.25 V. It should be noted that the thickness

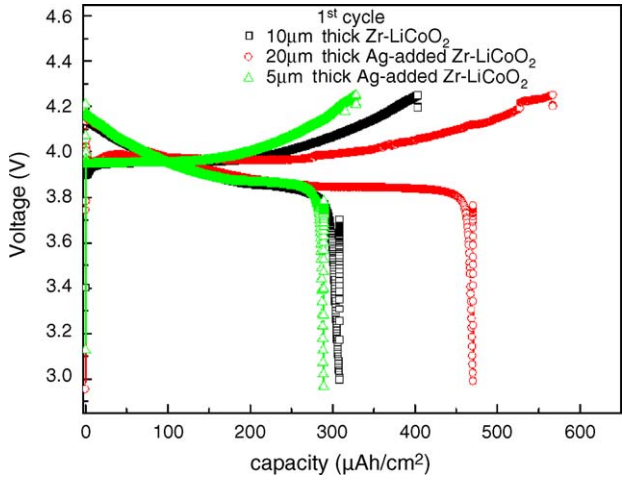

Fig. 4. Charge–discharge curves for Zr–$LiCoO_2$ and Ag-doped Zr–$LiCoO_2$ films. Note that the film thicknesses are different.

of each film is different. The discharge capacity per unit area tends to be larger for the thicker film. It appears, however, that the capacity of the 10 μm-thick Zr–$LiCoO_2$ film is about same as that of the thinner Ag-doped film.

The differential capacity (dQ/dV) versus voltage plots for the second cycle of the same cells (Fig. 4) are presented in Fig. 5. A large peak at around 3.9 V is seen for charge/discharge reactions. The peaks for Zr–$LiCoO_2$ are broad and their is large, whereas the peaks for Ag-doped samples are sharp with a small separation, even for the thicker film and, especially, in the case of the thinner film with 5 μm thickness, the peaks are very sharp. It is found that Ag addition reduces the polarization related to Li intercalation and de-intercalation kinetics, which leads to greater capacity. This is attributed to a decrease in film or inter-particle resistance that is induced by Ag particles added to the film. A further improvement in electrode performance with Ag particle addition is seen in the charge–discharge efficiency during cycling,

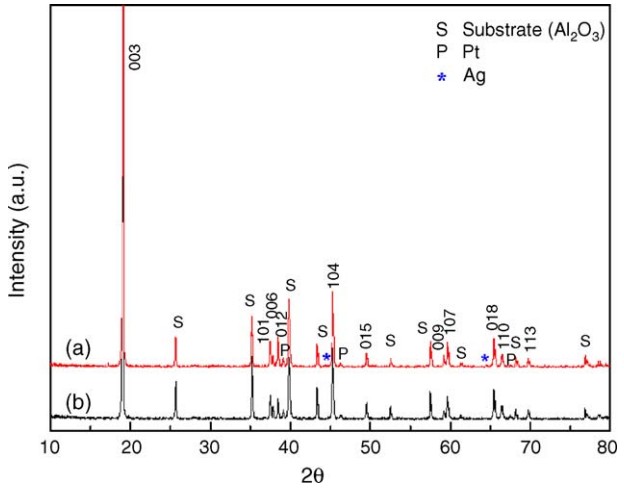

Fig. 3. X-ray diffraction patterns for screen-printed: (a) Zr–$LiCoO_2$; (b) Ag-doped Zr–$LiCoO_2$ after post-heat treatment.

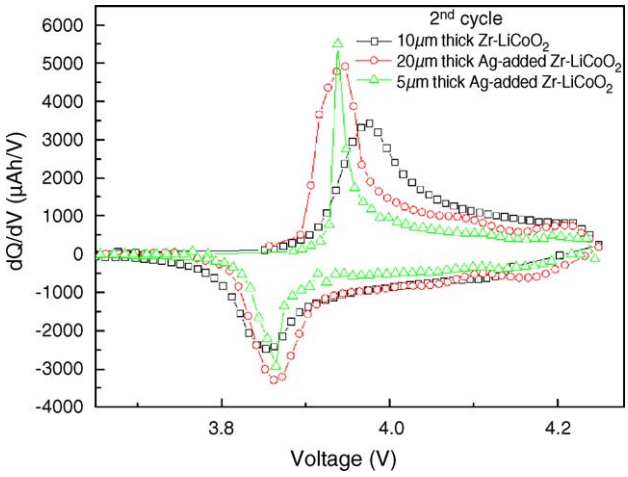

Fig. 5. Differential capacity vs. potential for second charge–discharge of same electrodes as in Fig. 4.

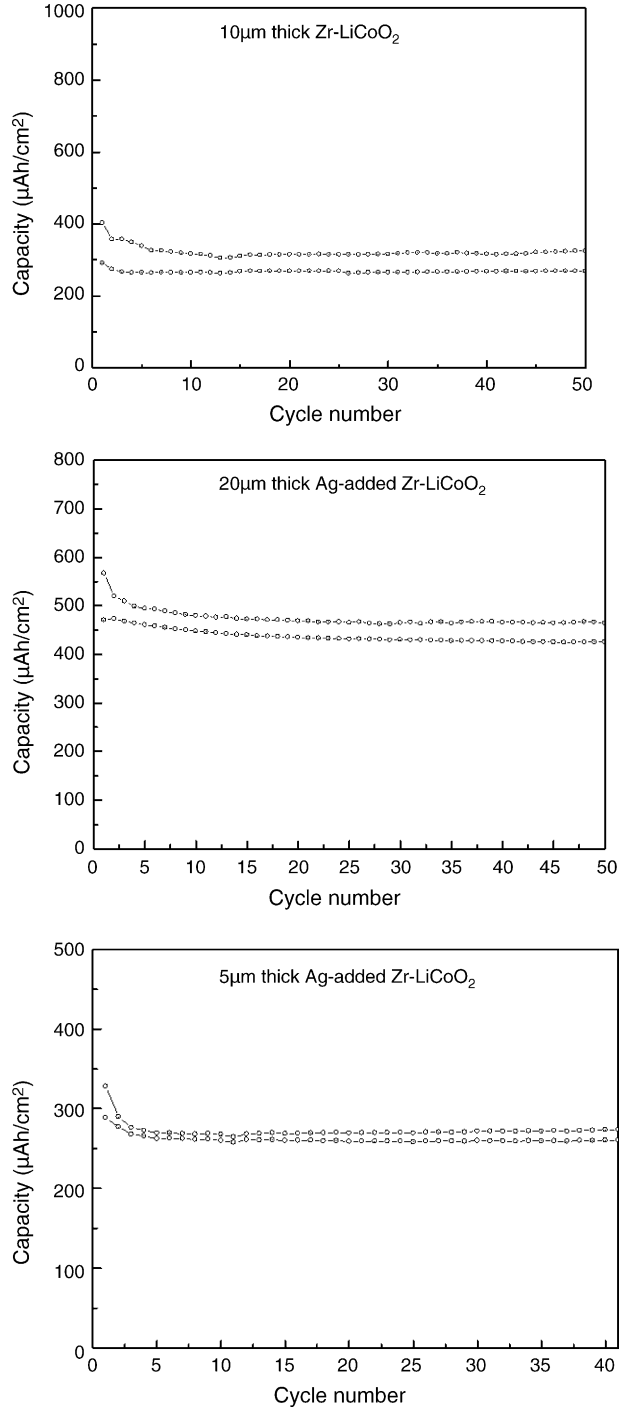

Fig. 6. Charge–discharge capacity vs. cycle number for selected film electrodes.

as shown in Fig. 6. The films exhibited a stable cycle performance but the charge–discharge efficiency is improved by Ag addition to film and decreasing film thickness. The coulombic efficiency of the 5 μm-thick Ag-doped film is above 96% for each cycle (Fig. 7). As illustrated in Fig. 8, however, the degree of utilization of the electrode material decreases with increasing film thickness, even for the Ag-doped films.

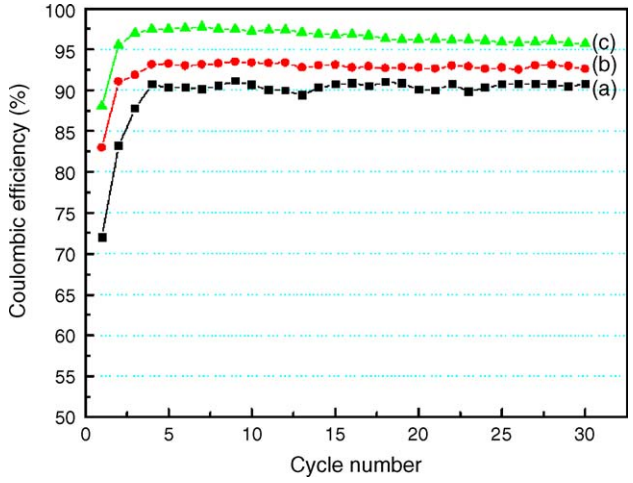

Fig. 7. Coulombic efficiencies of screen-printed film electrodes as function of cycle number: (a) 10 μm thick Zr–$LiCoO_2$ film, (b) 20 μm thick Ag-doped Zr–$LiCoO_2$ film and (c) 5 μm thick Ag-doped Zr–$LiCoO_2$ film.

The full cell of Zr–$LiCoO_2$ film/Fe–Si multilayer was examined. The multilayer films consisting of Si and Fe metal elements have been previously investigated [18] as anodes for lithium rechargeable batteries. The multilayer film used in this work was prepared by successive deposition of Si and Fe layers on to a Ni foil. It has a contact structure of Ti(150 Å)/Si(1500 Å)/Fe(100 Å)/Si(1500 Å)/Fe(100 Å)/Si(500 Å)/Fe(100 Å)/in which a Ti layer is deposited as an adhesion-promoting layer to enhance the adhesion between the Si layer and Ni substrate. The charge–discharge curves of the Li metal/Fe/Si multilayer film cell at constant current of 100 μA cm^{-2} between 0 and 1.2 V are presented in Fig. 9. The discharge capacity on the first cycle reaches 274 μAh cm^{-2}.

The charge and discharge capacities of the cell as a function of cycle number are shown in Fig. 10. There is a good cycleability, though gradual capacity fading occurs after about 30 cycles.

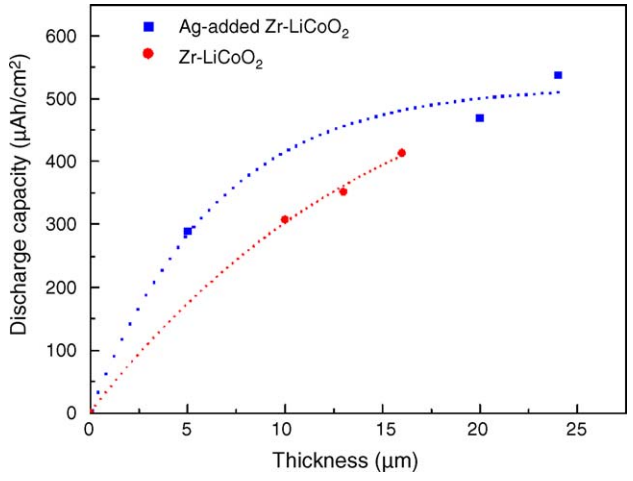

Fig. 8. Discharge capacity of screen-printed Zr–$LiCoO_2$ and Ag-doped Zr–$LiCoO_2$ film electrodes as function of film thickness.

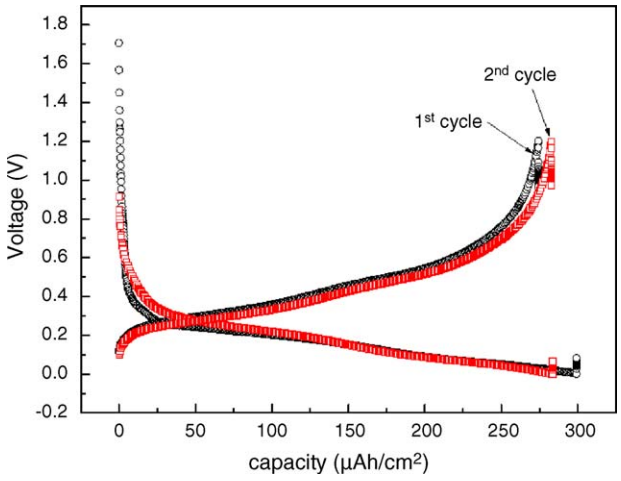

Fig. 9. Charge–discharge curves between 0 and 1.2 V at 100 μA cm^{-2} for the Fe/Si multilayer film for the first two cycles.

Considering the reversible capacity of the anode and cathode films measured by each half-cell test, the full cell was cycled as follows. A fixed quantity of charge (250 μAh cm^{-2}) was extracted from the cathode in each cycle and then inserted into the cathode until the cell voltage reached 2 V. The resulting charge–discharge potential profiles are plotted in Fig. 11. The overall cell voltage is slightly lower than that of the cell with the Li-metal anode, as can be deduced from the potential profile for the half-cell using a Fe/Si multilayer, shown in Fig. 9. From the data in Fig. 11, it can also be seen that the end-voltage for the cut-off capacity (250 μAh cm^{-2}) increases slightly. This is probable due to initial irreversible reactions at the anode and the cathode. In subsequent cycles, the end-voltage remains constant. The cycle performance of the full cell is given in Fig. 12. Excellent cycleability is obtained and the coulombic efficiency is about 85% for the first cycle and above 90% for the following cycles.

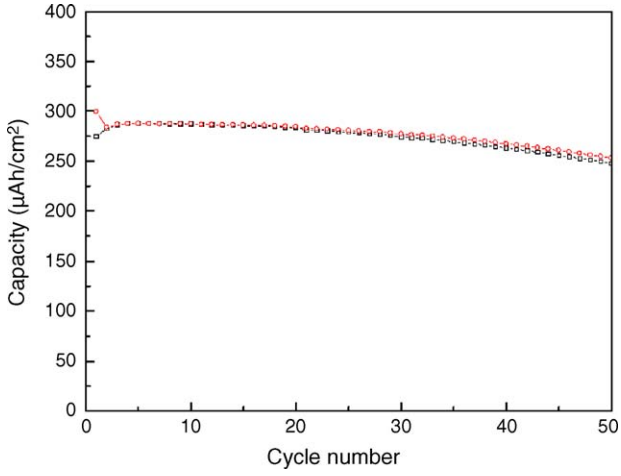

Fig. 10. Charge–discharge capacity vs. cycle number for Fe/Si multilayer film electrode.

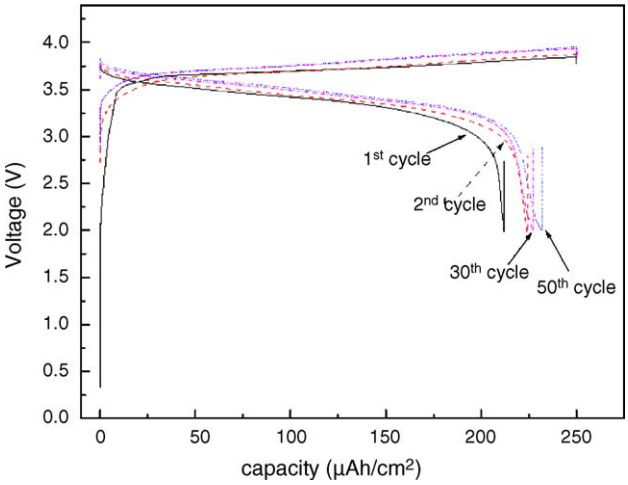

Fig. 11. Charge–discharge curves for full cell consisting of Fe/Si multilayer thin film anode and screen-printed Ag-doped Zr–$LiCoO_2$ film cathode.

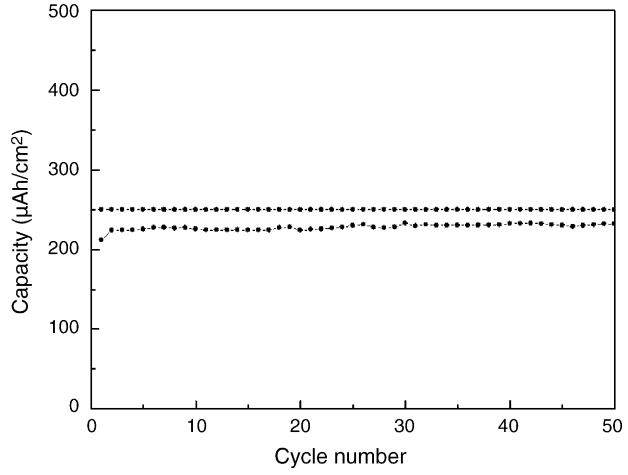

Fig. 12. Cycling performance for Fe–Si multilayer film/Ag-added Zr–$LiCoO_2$ cell.

4. Conclusion

The feasibility of preparing Zr–$LiCoO_2$ thick films up to 20 μm as the cathode material for lithium rechargeable batteries by screen-printing technique is demonstrated. The coating medium is a sol slurry that consists of Zr–$LiCoO_2$ sol and Zr–$LiCoO_2$ powder. After thermal treatment at 750 °C, crack-free thick films are obtained. Incorporation of 5 wt.% Ag powder into the sol slurry improves the electrochemical performance in terms of the charge–discharge efficiency during cycling. Excellent cycleability is obtained. As the film thickness increases, however, the degree of utilization of electrode material decreases.

Acknowledgments

This work was supported by the Korean Ministry of Science and Technology through the research program of the

‘National Research Laboratory’, and was also supported, in part, by LG Chemical Ltd.

References

[1] S.D. Jones, J.R. Akridge, J. Power Sources 54 (1994) 357.
[2] J.B. Bates, N.J. Dudney, D.C. Lubben, G.R. Gruzalski, B.S. Kwak, X. Yu, R.A. Zuhr, J. Power Sources 54 (1995) 58.
[3] Y.S. Park, S.H. Lee, B.I. Lee, S.K. Joo, Electrochem. Solid State Lett. 2 (1999) 58.
[4] N.J. Dudney, B.J. Neudecker, Curr. Opin. Solid-state Mater. Sci. 4 (1999) 479.
[5] J.B. Bates, N.J. Dudney, B.J. Neudecker, A. Ueda, C.D. Evans, Solid State Ionics 135 (2000) 33.
[6] J.L. Souquet, M. Duclot, Solid State Ionics 148 (2002) 375.
[7] N.J. Dudney, Y.I. Jang, J. Power Sources 119–121 (2003) 300.
[8] B. Wang, J.B. Bates, F.X. Hart, B.C. Sales, R.A. Zuhr, J.D. Robertson, J. Electrochem. Soc. 143 (1996) 3203.
[9] J.K. Lee, S.J. Lee, H.K. Baik, H.Y. Lee, S.W. Jang, S.M. Lee, Electrochem. Solid State Lett. 2 (1999) 512.
[10] J.F. Whitacre, W.C. West, B.V. Ratnakumar, J. Power Sources 103 (2001) 134.
[11] J.B. Bates, N.J. Dudney, B.J. Neudecker, F.X. Hart, H.P. Jun, S.A. Hackney, J. Electrochem. Soc. 147 (2000) 59.
[12] C.-L. Liao, K.-Z. Fung, J. Power Sources 128 (2004) 263.
[13] J. Pracharova, J. Pridal, J. Bludska, I. Jakubec, V. Vorlicek, Th. Dikonimos Makris, R. Giorgi, L. Jastrabik, J. Power Sources 108 (2002) 204.
[14] C.N. Polo da Fonseca, J. Davalos, M. Kleinke, M.C.A. Fantini, A. Gorenstein, J. Power Sources 81/82 (1999) 575.
[15] P. Fragnaud, T. Brousse, D.M. Schleich, J. Power Sources 63 (1996) 187.
[16] W.S. Kim, J. Power Sources 134 (2004) 103.
[17] K.J. Rao, H. Benqlilou-Moudden, G. Couturier, P. Vinatier, A. Levasseur, Mater. Res. Bull. 37 (2002) 1353.
[18] Y.I. Jang, Ncancy J. Dudney, Duglas A. Blom, Allard L.F. Lawrence, J. Power Sources 119–121 (2003) 295.
[19] M. Antaya, K. Cearns, J.S. Preston, J.N. Reamers, J.R. Dahn, J. Appl. Phys. 76 (1994) 2799.
[20] Y. Iriyama, M. Inaba, T. Abe, Z. Ogumi, J. Power Sources 94 (2001) 175.
[21] M.K. Kim, H.T. Chung, Y.J. Park, J.G. Kim, J.T. Son, K.S. Park, H.G. Kim, J. Power Sources 99 (2001) 34.
[22] Y.H. Rho, K. Kanamura, M. Fujisaki, J. Hamagami, S. Suda, T. Umegaki, Solid State Ionics 151 (2002) 151.
[23] P.J. Holmes, R.G. Loasby, Handbook of Thick Film Technology, Electrochemical Publication Limited, 1976.
[24] J.B. Kim, H.Y. Lee, K.S. Lee, S.H. Lim, S.M. Lee, Electrochem. Commun. 5 (2003) 544.
[25] A. Choblet, H.C. Shiao, H.-P. Lin, M. Salomon, V. Manivannan, Electrochem. Solid State Lett. 4 (2001) A65.